Contents lists available at ScienceDirect

Arabian Journal of Chemistry

journal homepage: www.sciencedirect.com

Original article

Aligned carbon nanofibers-guided bone regeneration and orthopedic applications: A pilot study

Jingzhe Zhang [a], Xinkun Wang [a], Xinbiao Fu [a], Ye Li [a,*], Rubo Li [b]

[a] Department of Orthopedics, the Third Clinical Hospital of Jilin University, Changchun 130000, China
[b] Department of Surgery, Shijiazhuang Fifth Hospital, Shijiazhuang 050000, China

ABSTRACT

In the present study, we fabricated electroconductive aligned carbon nanofibers (CNFs) as the nanofibers-guided bone regeneration scaffold. The CNFs were obtained from electrospun polyacrylonitrile nanofibers through two steps heat treatment. Aligned nanofibers were fabricated at high drum speed (2400 rpm). The fabricated CNFs were characterized regarding the morphology, crystallinity, carbon structure, wettability, electrical conductivity, hemocompatibility, cytocompatibility, and cell morphology. The results showed that the nanofibers obtained at 2400 rpm drum speed were aligned and electrical conductivity was dependent on the direction of conductivity measurement. The highest electrical conductivity (3.92 0.09 S.cm^{-1}) was obtained at the measuring direction of that parallel to the axis of CNFs. The in vitro studies confirmed that the CNFs induced negligible hemolysis, indicating the hemocompatibility of CNFs. The cell viability assessment showed the biocompatibility of CNFs. The cell SEM images showed that MG-63 cells (an osteoblast-like cell line) were grown at a direction that parallels the axis of aligned CNFs, while the growth on the random CNFs was without a specific pattern. In conclusion, this study indicates that the fabricated aligned CNFs can be considered and the nanofibers-guided bone regeneration scaffold.

© 2023 The Authors. Published by Elsevier B.V. on behalf of King Saud University. This is an open access article under the CC BY license (http://creativecommons.org/licenses/by/4.0/).

1. Introduction

Bone large fractures and defects required interventions to properly heal. Bone autografts are the gold standard in these conditions and despite positive healing outcomes, have some significant limitations. For instance, secondary surgery and patient discomfort, limited source, graft resorption, infection, and donor site morbidity (Kim et al., 2020; Burg et al., 2000; Brown and Laurencin, 2020). Therefore, innovative approaches, such as tissue engineering have been evolving last years as an alternative to circumvent these limitations. Biomaterials and scaffolds have central roles in tissue engineering applications as the substrate for cell attachment, growth, migration, and differentiation. Moreover, the functional scaffolds can bear drugs and act as the carrier for local drug delivery. In this regard, unprecedented efforts have been conducted to develop bioactive and functional scaffolds with desired properties for bone tissue engineering applications (Bose et al., 2012; Qu et al., 2019). Various types of structures have been evaluated as the scaffold for bone regeneration, such as hydrogels, 3D printed constructs, thermal-induced phase-separated scaffolds, nanofibers, and hybrid structures. Among them, nanofibers have shown fascinating and promising properties beneficial for bone tissue engineering (Madrid et al., 2019; Qu, 2020).

Nanofibers have a high specific surface-to-volume ratio proper for cell attachment, the highest morphological similarity to the extracellular matrix (ECM), and the possibility to load various bioactive factors into/on nanofibers. Various fabrication methods have been developed for nanofibers production, such as drawing, template assist, self-assembly, phase separation, and electrospinning (Subbiah et al., 2005; Ramakrishna et al., 2006). Electrospinning is a sophisticated technique enabling researchers/companies to fabricate nanofibers with a variety of morphologies, arrangements, and architectures from different sources of materials (Yang et al., 2020; Liu et al., 2020; Guo et al., 2021; Jiang et al., 2018). Various polymeric solution (e.g. concentration, viscosity, and electrical conductivity), environmental (e.g. temperature, humidity, atmosphere), and working (e.g. applied voltage, feeding

* Corresponding author at: The Third Clinical Hospital of Jilin University, No.126, Xiantai Street, Changchun 130000, China(Ye Li)
E-mail address: lye99@jlu.edu.cn (Y. Li).

Peer review under responsibility of King Saud University.

Production and hosting by Elsevier

rate, nozzle to collector distance, and drum speed) parameters are involved in this technique, which can be controlled to tune the properties of the final nanofibers (Subbiah et al., 2005; Bhardwaj and Kundu, 2010).

The coordination between the properties of the designed/fabricated scaffold with the native tissue along with biocompatibility are the key factors of a successful tissue engineering scaffold. Bone is an electroactive tissue and contains a complex electrical system modulating bone cell's functions and bone mass density (Cui et al., 2020; Wibowo et al., 2020). These biological electrical fields have determinant roles in the proliferation, signaling, orientation, morphology, migration, and regenerative processes of bone cells. According to this scenario, electroconductive scaffolds and electrical stimulation have been utilized in bone tissue engineering to modulate bone cells functions and promote bone tissue regeneration. The development of electroconductive scaffolds that enable us to deliver electrical, electromechanical, or electrochemical stimulations locally/directly/controlled to the target cells, tissue, and organs is an unprecedented breakthrough in the bone regeneration field. Different electroconductive materials have been utilized for fabricating scaffolds, such as conductive polymers (Hardy et al., 2013; Lee, 2013; Balint et al., 2014), metallic-based (Wickham et al., 2016; Baei et al., 2016; Nguyen et al., 2016; Baranes et al., 2016), and carbon-based materials (Zhang et al., 2018; Wang et al., 2019; Huang et al., 2019; Martins et al., 2014). Among them, carbon-based structures, especially electrospun carbon nanofibers (CNFs), have fascinating properties regarding the electrical conductivity, mechanical strength, and biocompatibility. Generally, electrospun CNFs are obtained from precursor polymeric nanofibers, such as polyacrylonitrile (PAN), polyamic acid, Copolyacrylonitrile (coPAN), etc. Among them PAN has attracted significant attention due to higher carbonization yield and proper mechanical properties (Duan et al., 2018; Xu et al., 2021). Accordingly, CNFs can serve as a sophisticated structure with promising performance in tissue engineering applications. Compared with other electros conductive polymers (Polyaniline, Polypyrrole, poly(3,4-ethylenedioxythiophene), and polythiophene, electrospun CNFs are more biocompatible and have excellent mechanical properties.

The topography and architecture of scaffolds have determinant roles in the functions and behavior of cells, and subsequently the outcomes of the tissue engineering strategy. It has been shown that aligned nanofibers can alter cell morphology, functions, and migration direction (Macossay-Torres et al., 2015). Xu et al. (Xu et al., 2004) reported that the human coronary artery smooth muscle cells migrate along the axis of the aligned poly(L-lactide-co-caprolactone) and exhibit a spindle-like contractile phenotype. In another study, Yin et al. (Yin, 2010) showed that tendon progenitor cells differentiated to teno-lineage and showed spindle-shaped morphology on the aligned poly(L-lactic acid) nanofibers. Although there are other studies evaluating the effects of polymeric nanofibers on the morphology of the cells, this is the first report on the assessing of CNFs morphology on bone cell and proposing the structure for bone tissue engineering. Therefore, in the present study, we combine the electrical conductivity and biocompatibility of electrospun CNFs with their aligned morphology as the tuned bone engineering scaffold.

2. Materials and methods

2.1. Reagents

Polyacrylonitrile (PAN, average Mw 150,000), N,N-Dimethylformamide (DMF), Sodium hydroxide (NaOH), Paraformaldehyde (PFA), and dimethyl sulfoxide (DMSO) were purchased from Merck (Darmstadt, Germany). DMEM/F-12 cell culture medium, Trypsin-EDTA, FBS (Fetal Bovine Serum), and Pen-Strep(Penicillin-Streptomycin) were obtained from Gibco (Germany). Cell Proliferation Kit I (MTT) was purchased from Roth (Germany).

2.2. CNFs fabrication

For the CNFs fabrication (random and aligned), PAN/DMF solution with a concentration of 12 wt% was prepared and stirred for 24 h to obtain a clear and homogenous solution. The prepared solution was converted to nanofibers using a commercial electrospinning apparatus. The electrospinning parameters for random PAN nanofibers fabrication were the applied voltage of 20 kV, the feeding rate of 1 mL/h, nozzle to collector distance of 10 cm, and drum speed of 400 rpm. For the aligned PAN nanofibers, the parameters were the same except the drum speed, which was 2400 rpm. The high speed of the drum is the main driving force of fabricating the aligned nanofibers. The prepared random and aligned PAN nanofibers were converted to CNFs through two steps heat treatment, the stabilization of PAN polymer chains at 280 °C for 2 h in an air atmosphere and the carbonization of the PAN polymer chains at 1000 °C for 1 h in N_2 atmosphere. The fabricated CNFs were treated with concentrated NaOH at 50 °C for 12 h to induce OH groups on CNFs and increase the hydrophilicity on CNFs. During the stabilization process, the ringing of the nitrile groups of PAN and polymerization of polymer chains takes place and during the carbonization process, non-carbonaceous substances remove, dehydrogenation and denitrogenation take place, and ladder-like structures form. It is reported that CNFs obtained from PAN have a carbon yield of 85%, which is considerable (Jadhav et al., 2019).

2.3. Morphological evaluations

Scanning Electron microscopy (SEM) was used to observe the morphology of the fabricated random and aligned PAN and CNFs. A piece of the nanofibrous mat was cut (0.5 × 0.5 cm), sputter-coated with a thin layer of gold using a sputter coater (SCD 004, Balzers, Germany) to increase the conductivity, and imaged using SEM apparatus (Philips XL-30) at the acceleration voltage of 25 kV and the working distance of 13.6 mm. Image J software (1.47v, National Institute of Health, USA) was applied to measure and calculate the diameter of the nanofibers.

2.4. Crystallinity assessment

X-ray diffraction (XRD) analysis was conducted to assess the crystallinity of the fabricated CNFs. The experiment was performed using an x-ray diffractometer (PHILIPS-PW1730, Cu-Kα origin (λ = 1.540598 A○) and Bragg angle (2θ) of 5°–60°.

2.5. Microstructure evaluation

Raman spectroscopy is the standard method to evaluate the microstructure and molecular morphology of carbonaceous substances. The disorders and structural quality of carbonaceous substances can be revealed according to D-band and G-band in the Raman spectra. The Raman spectroscopy was conducted using a Raman spectrometer (Teksan Takram P50C0R10 Raman spectrometer with the laser power of 0.5–70 mW and laser wavelength of 532 nm.

2.6. Wettability measurement

The hydrophilic/hydrophobic nature of the prepared CNFs was investigated using the water contact angle (WCA) method. The analysis was performed using a camera-equipped goniometer

(VCA-optima, AST). In this analysis, three deionized water droplets (0.25 µL) were dropped on different places of the samples and imaged three second later. The image of the droplets was captured and analyzed. It is well-known that the WCA lower than 90° is considered as the hydrophilicity and the WCA higher than 90° as the hydrophobic surface.

2.7. Electroconductivity assessment

Electric Conductivity is important for scaffolds designed for electroactive tissues. A standard four-point probe multimeter (Signatone SYS-301 with Keithley196 system DDM multimeter) was used to measure the electrical conductivity of the prepared CNFs. The electrical conductivity of the prepared aligned CNFs was measured in two directions, in the directions perpendicular and parallel to the CNFs axis to assess the effects of fibers alignment on the electrical conductivity.

2.8. In vitro studies

2.8.1. Hemocompatibility investigation

The hemolysis induced by the prepared random and aligned CNFs was assessed as the indication of hemocompatibility. Fresh anticoagulated blood was diluted with phosphate-buffered saline (PBS, pH: 7.4) and incubated with 100 mg of the CNFs at 37° C for 1 h. The incubated blood was centrifuged (10 min at 1500 rpm) and the absorbance of the supernatant was read at 545 nm using the Microplate Reader. The experiment was conducted in triplicate and the absorbance values ± standard deviation were reported. Positive control: RBC lyzed with DI water, Negative control: RBC treated with PBS.

2.8.2. Cell viability measurement

The viability of MG-63 cells (osteoblast-like cells) on the prepared random and aligned CNFs was measured using the MTT assay kit. The MTT assay is a quantitative experiment measuring the metabolic activity of the cells as an indication of cell viability. Viable cells convert the MTT salt to formazan crystals and the absorbance of dissolved crystals (using DMSO) is correlated to metabolic activity and subsequently viability of the cells. For the experiment, random and aligned CNFs were punched circulatory, put on the bottom of 96-wells calculate plate. The CNFs were sterilized using ethanol for 24 h and washed with sterilized PBS (pH: 7.4) several times. A number of 5,000 cells in 100 µL DMEM cell culture medium containing PBS (10 % v/v) and Pen/Strep was incubated with CNFs for 3 and 5 days in a humidified cell culture incubator at 37 °C with CO_2 (5%). The cell culture medium was replaced with a fresh one every other day. After the incubation times, the cell culture medium was aspirated, the cells were washed with sterilized PBS (pH: 7.4) three times and incubated with MTT salt (0.5 mg mL^{-1}) for 4 h. The formed formazan crystals were dissolved using 200 µL DMSO and the absorbance read at 570 nm using a Microplate Reader.

2.8.3. Cell morphology on CNFs

Cells are able to sense the topography of the scaffold and response to the substrate. Therefore, assessing the morphology of cells on the cultured scaffolds provide informative results. The morphology of MG-63 cells on the prepared random and aligned CNFs was observed using SEM imaging after fixation and dehydration. The CNFs were sterilized and seeded according to the MTT protocol and incubated for 5 days. Then, the cell culture medium was removed, the cells washed with PBS, and fixed using PFA 4% in PBS for 60 min at 4 °C. The fixed cells were dehydrated using graduated ethanol, sputter-coated with a thin layer of gold and observed at 20.0 kV accelerating voltage. For the DAPI staining,

the cells seed and fixed according to the above-mentioned protocol, then the cells membrane was permeable using triton x100 (60 µL) for 10 min and stained using 50 µL DAPI stain diluted in PBS (1: 1,000), The cells were observed and imaged under fluorescent microscopy.

2.9. Statistical analysis

The experiments were performed in triplicate except the MTT assay and hemolysis measurement, that was conducted on five samples in each group. The one-way analysis of variance (ANOVA) and Tukey's multiple comparison test ($p < 0.05$) using SPSS program, v.23 (IBM, Armonk, NY, USA) by applying.

3. Results and discussion

3.1. Morphology of nanofibers

The morphology of the fabricated random and aligned PAN and PAN-derived CNFs was observed using SEM imaging after coating with a thin layer of gold. As shown in Fig. 1, the random orientation (Fig. 1A) and aligned orientation (Fig. 1B) PAN nanofibers are apparent. The corresponding CNFs also have random (Fig. 1C) and aligned (Fig. 1D) ordination. These observations indicate that it is possible to fabricate aligned CNFs from aligned PAN nanofibers. Although there are some deformations and fusions between the random and aligned CNFs, which are due to the conducted heat treatments. The nanofibers diameter measurement using the Image J software showed that the random PAN nanofibers have a diameter of 233 ± 51 nm and aligned PAN nanofibers have a diameter of 201 ± 43 nm. The difference between the diameter of random and aligned PAN nanofibers can be related to the difference of drum speed during the electrospinning process, which at high speed (2400 rpm for aligned condition) stretches the nanofibers and slightly reduces the aligned nanofibers diameter. The random and aligned CNFs diameter were 210 ± 40 and 196 ± 42 nm, respectively. The smaller diameter of CNFs compared to the corresponding PAN nanofibers is due to the heat treatment process, which shrinks the nanofibers diameter and removal of noncarbonaceous substances of PAN precursor. The wettability assessment showed that the water contact angle value of random and aligned CNFs were 92.3 ± 5.0 and 82.0 ± 6.1° respectively. The water contact angle measurement indicated that the wettability of the prepared CNFs is in the border of hydrophobicity/hydrophilicity. Carbon-based materials can be obtained from biomass and applied for biomedical applications (Jjagwe et al., 2021; Zheng et al., 2021; Lou et al., 2019). According to the literature, we estimate that we obtained a carbon yield of 80–85% (Jadhav et al., 2019).

3.2. Crystallinity test

The crystallinity of the prepared CNFs was evaluated using XRD analysis, the informative method revealing the crystal nature of structures. As shown in Fig. 2. the peaks observed at 2θ = 26° and 2 θ = 44° are related to the (0 0 1) and (0 0 2) crystalline planes of the prepared CNFs, respectively, revealing the partial crystalline nature of the CNFs. Moreover, the quantitative data obtained using Xpert Highscore Software showed that the full width at half maximum (FWHM) value for the CNFs is about 0.19 and the B (radian) of 0.003.
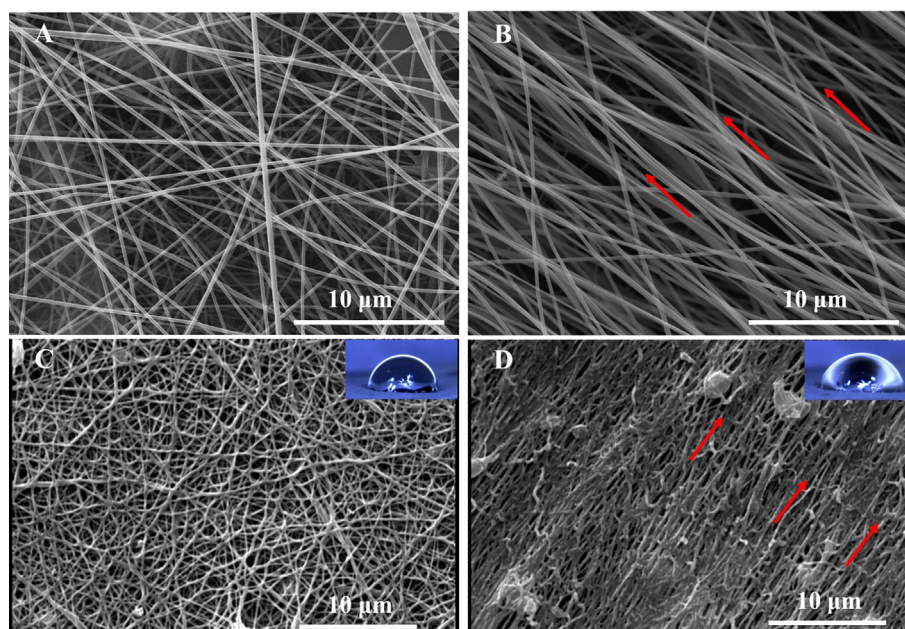
Fig. 1. SEM micrograph of (A) random PAN nanofibers, (B) aligned PAN nanofibers, (C) random CNFs, and (D) aligned CNFs. Red arrows indicate direction of alignment.

3.3. Raman results

Raman spectroscopy is the standard method of analyzing carbon-based structures and is conducted to assess the microstructure of the fabricated CNFs. The peaks located at 1250–1450 cm^{-1} are related to the D-band indicating disorder-induced phonon mode and the peak located at 1550–1660 cm^{-1} is attributed to the G-band indicating the graphite band in the structure of the fabricated CNFs (data not shown). Moreover, the presence of disordered and defective portions of carbon in the CNFs can be revealed through the D-band and the graphitic crystallites of carbon can be indicated through the G-band. Moreover, the "R-value" (R = ID/IG) is an informative value representing the degree of disorder in CNFs structure. The R-value for the fabricated CNFs around is 0.94 and revealed that the fabricated random and aligned CNFS structures are the combinations of nanocrystalline graphite in the base of amorphous carbon as revealed by other studies (Ji et al., 2009; Kim et al., 2006).

3.4. Electrical conductivity

Electroconductive scaffolds have promising roles in bone regeneration and their electrical conductivity should be assessed. The electrical conductivity of the prepared random and aligned CNFs was measured in two directions, in the directions perpendicular and parallel to the CNFs axis to assess the effects of fibers alignment on the electrical conductivity. The electrical conductivity of random CNFs is the two directions were 2.15 ± 0.04 S.cm^{-1} and 2.20 ± 0.03 S.cm^{-1}. On the other hand, the electrical conductivity aligned in the directions perpendicular to the CNFs axis was 1.80 ± 0.02 S.cm^{-1} while in the direction parallel to the axis was 3.92 0.09 S.cm^{-1}. The significantly ($p < 0.05$) higher electrical conductivity in the direction parallel to the axis of CNFs can be due to the fact that the aligned CNFs provide a good conducting pathway. These observations are in agreement with the previous studies. Gu et al. (Gu et al., 2018) reported that the electrical conductivity of aligned chitin/polyaniline nanofibers was about 91% higher than the random nanofibers. In another study, Subramanian et al. (Subramanian et al., 2012) reported that the electrical conductivity
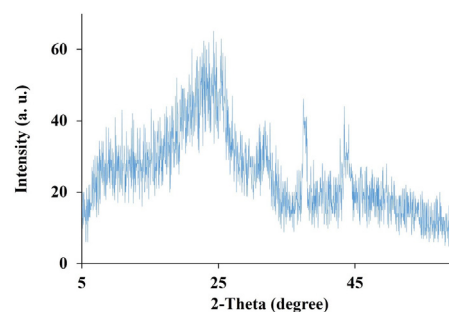

Fig. 2. The XRD pattern of the prepared CNFs.

of aligned poly(lactide-co-glycolide)/poly(3-hexylthiophene) was significantly higher than the randomly oriented nanofibers.

3.5. Hemocompatibility investigation

Hemocompatibility is a vital requirement for structures dedicated to being in contact with blood components. Hemolysis induced by the fabricated scaffolds can be an indication of the hemocompatibility of the scaffolds. As shown in Fig. 3, the hemolysis induced by the fabricated random and aligned CNFs is significantly lower than the positive control group ($p < 0.05$). These results indicate that the prepared random and aligned CNFs are hemocompatible, which came from the chemical inertness and biocompatibility of the nanofibers.

3.6. Cell proliferation results

The proliferation of MG-63 cells on the fabricated random and aligned CNFs was measured using the MTT assay kit. As shown in Fig. 4, the fabricated random and aligned CNFs did not induce adverse effects on the cells growth and promote the proliferation of cells. Moreover, the proliferation of MG-63 cells on the aligned CNFs was higher than the control (tissue culture plastic) and the random CNFs. Gu et al. (Gu et al., 2018) also observed higher cell proliferation on the aligned nanofibers and reported that the cell
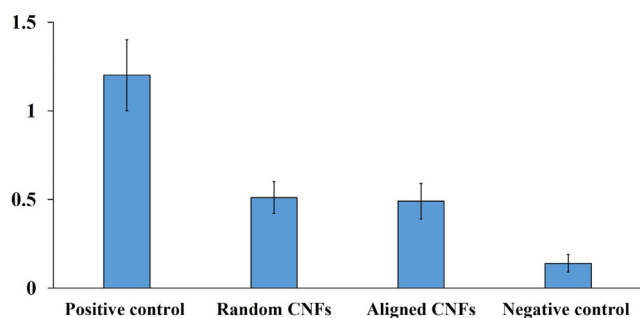
Fig. 3. Hemolysis induced by the fabricated random and aligned CNFs. Positive control: RBC lyzed with DI water, Negative control: RBC treated with PBS. Values represent the mean ± SD, n: 5, * p < 0.05, (obtained by one-way ANOVA).

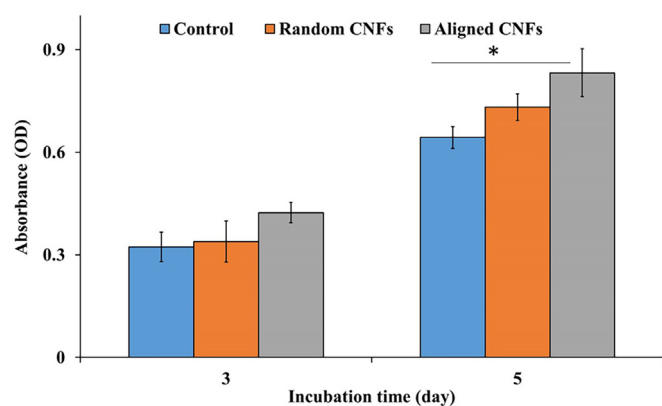**Fig. 4.** MG-63 cells viability/proliferation on the fabricated random and aligned CNFs. Values represent the mean ± SD, n: 5, * p < 0.05, (obtained by one-way ANOVA).

proliferation was 2.1-fold higher than that for the random nanofibers. They concluded that the aligned nanofibers provide a higher-affinity surface for cell proliferation than the random nanofibers. Lee et al. (Lee et al., 2014) observed that the proliferation of mesenchymal stem cells (hMSCs) on aligned PLLA nanofibers was higher than the random orientation one and the cells migration along the parallel direction of the nanofibers axis was 10.46-fold faster than in the perpendicular direction. These observations indicate that the aligned nanofibers not only are beneficial for cell attachment but also facilitate the migration of cells.

3.7. Cell attachment and morphology on CNFs

The attachment and morphology of MG-63 cells on the prepared random and aligned CNFs were evaluated using DAPI stain-

ing and SEM imaging, respectively. DAPI is a fluorescent stain applied to the nucleus of cells through the binding to A-T-rich regions in DNA. The observed blue fluorescent color indicates the cells on the intended scaffold. As shown, in Fig. 5A, B, the attachment of MG-63 cells on the prepared random and aligned CNFs are apparent.

The morphology of MG-63 cells on the prepared random and aligned CNFs was observed using SEM imaging after fixation, dehydration, and sputter coating with gold. As shown in Fig. 6A, MG-63 cells exhibited irregular morphology on the prepared random CNFs. On the other hand, the growth of MG-63 cells on the prepared aligned CNFs is in the direction parallel to the axis of CNFs (Fig. 6B). These results imply that using aligned CNFs it is possible to guide the cell growth in the desired direction. Lee et al. (Lee et al., 2014) reported that using aligned nanofibers it is possible to modulate the cells growth and migration through providing spatial guidance for cells. The in vivo studies demonstrated that the direction of bone regeneration was consistent with the alignment of nanofibers and collagen fibrils orientation overlapped along the direction of nanofibers. These findings, stretching of the cells in the direction of the axis of aligned CNFs, indicate that the prepared CNFs support nanofibers-guided bone regeneration.

4. Conclusion

Tissue engineering is highly dependent on scaffolds and their physicochemical and morphological features. Cells can sense environmental stimuli and respond to the stimuli. Physical stimuli in the form of scaffolds/substrates could modulate the morphology and functions of cells. It has been shown that nanofibers' orientation affects cell behavior, and several studies have aimed to evaluate these correlations. In the current study, we aimed to combine nanofibrous morphology, biocompatibility, and electrical conductivity of electrospun CNFs with their aligned orientation to develop nanofibers-guided bone regeneration concept. The results showed that the aligned PAN nanofibers were fabricated at a drum speed of 2400 rpm and the heat treatment steps have negligible effects on the nanofiber's alignment. Moreover, it was observed that the drum speed can reduce the diameter of the nanofibers due to the induced stretching force. It was observed that the nanofiber's alignment affects the electrical conductivity of nanofibers and the conductivity in the direction parallel to the axis of nanofibers was the highest. The fabricated random and aligned CNFs have the same composition. The in vitro studies revealed that the fabricated CNFs were hemocompatible, biocompatible, and support cell attachment. Moreover, it was observed that the CNFs alignment modulated the morphology and wroth direction of the cells. These findings indicate that CNFs have promising potential as bone tissue engineering scaffolds. For the future direction, the molecular mechanisms of cells' response to the alignment can be clarified. Moreover, the prepared aligned CNFs should be evaluated in the
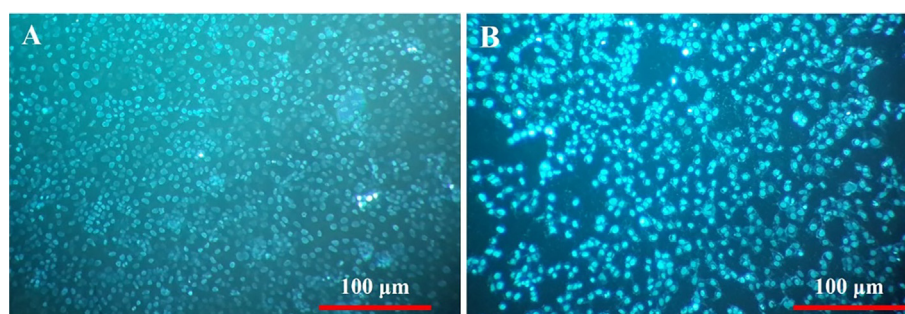

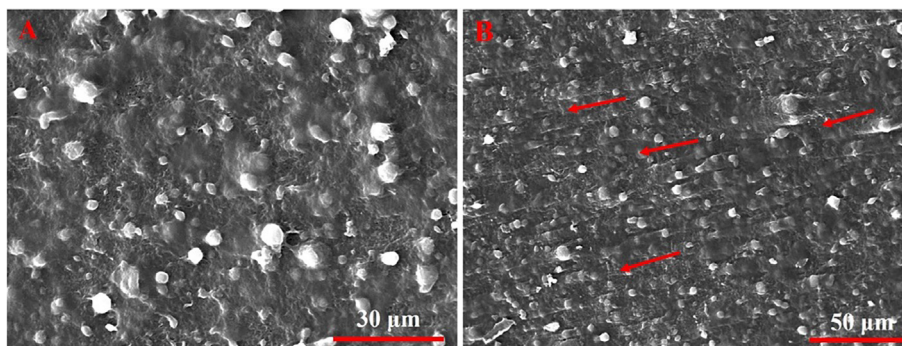**Fig. 5.** Cell attachment on the prepared (A) random and (B) aligned CNFs stained with DAPI.

Fig. 6. SEM micrograph of MG-63 cells cultured on (A) random and (B) aligned CNFs. The arrows indicate the direction of cell growth and CNFs alignment.

animal model and apply effective treatments on CNFs to make them biodegradable.

Declaration of Competing Interest

The authors declare that they have no known competing financial interests or personal relationships that could have appeared to influence the work reported in this paper.

References

Baei, P. et al., 2016. Electrically conductive gold nanoparticle-chitosan thermosensitive hydrogels for cardiac tissue engineering. Mater. Sci. Eng. C 63, 131–141.

Balint, R., Cassidy, N.J., Cartmell, S.H., 2014. Conductive polymers: Towards a smart biomaterial for tissue engineering. Acta Biomater. 10 (6), 2341–2353.

Baranes, K. et al., 2016. Gold nanoparticle-decorated scaffolds promote neuronal differentiation and maturation. Nano Lett. 16 (5), 2916–2920.

Bhardwaj, N., Kundu, S.C., 2010. Electrospinning: a fascinating fiber fabrication technique. Biotechnol. Adv. 28 (3), 325–347.

Bose, S., Roy, M., Bandyopadhyay, A., 2012. Recent advances in bone tissue engineering scaffolds. Trends Biotechnol. 30 (10), 546–554.

Brown, J.L. and C.T. Laurencin, Bone tissue engineering, in Biomaterials Science2020, Elsevier. p. 1373-1388.

Burg, K.J., Porter, S., Kellam, J.F., 2000. Biomaterial developments for bone tissue engineering. Biomaterials 21 (23), 2347–2359.

Cui, L. et al., 2020. Electroactive composite scaffold with locally expressed osteoinductive factor for synergistic bone repair upon electrical stimulation. Biomaterials 230, 119617.

Duan, G. et al., 2018. Microstructures and mechanical properties of aligned electrospun carbon nanofibers from binary composites of polyacrylonitrile and polyamic acid. J. Mater. Sci. 53 (21), 15096–15106.

Gu, B.K., Park, S.J., Kim, C.-H., 2018. Beneficial effect of aligned nanofiber scaffolds with electrical conductivity for the directional guide of cells. J. Biomater. Sci. Polym. Ed. 29 (7–9), 1053–1065.

Guo, H., et al., Electrospun fibrous materials and their applications for electromagnetic interference shielding: A review. Composites Part A: Applied Science and Manufacturing, 2021: p. 106309.

Hardy, J.G., Lee, J.Y., Schmidt, C.E., 2013. Biomimetic conducting polymer-based tissue scaffolds. Curr. Opin. Biotechnol. 24 (5), 847–854.

Huang, B. et al., 2019. Fabrication and characterisation of 3D printed MWCNT composite porous scaffolds for bone regeneration. Mater. Sci. Eng. C 98, 266–278.

Jadhav, S.A. et al., 2019. Brief overview of electrospun polyacrylonitrile carbon nanofibers: Preparation process with applications and recent trends. Mater. Des. Process. Commun. 1 (5), e83.

Ji, L., Medford, A.J., Zhang, X., 2009. Porous carbon nanofibers loaded with manganese oxide particles: Formation mechanism and electrochemical performance as energy-storage materials. J. Mater. Chem. 19 (31), 5593–5601.

Jiang, S. et al., 2018. Electrospun nanofiber reinforced composites: A review. Polym. Chem. 9 (20), 2685–2720.

Jjagwe, J. et al., 2021. Synthesis and application of Granular activated carbon from biomass waste materials for water treatment: A review. J. Bioresour. Bioprod.

Kim, C. et al., 2006. Fabrication of electrospinning-derived carbon nanofiber webs for the anode material of lithium-ion secondary batteries. Adv. Funct. Mater. 16 (18), 2393–2397.

Kim, T. et al., 2020. Orthopedic implants and devices for bone fractures and defects: Past, present and perspective. Eng. Regen. 1, 6–18.

Lee, J.Y., 2013. Electrically conducting polymer-based nanofibrous scaffolds for tissue engineering applications. Polym. Rev. 53 (3), 443–459.

Lee, J.-H et al., 2014. Guidance of in vitro migration of human mesenchymal stem cells and in vivo guided bone regeneration using aligned electrospun fibers. Tissue Eng. A 20 (15–16), 2031–2042.

Liu, L. et al., 2020. A review of smart electrospun fibers toward textiles. Compos. Commun. 100506

Lou, Z. et al., 2019. Fabrication of Fe/C composites as effective electromagnetic wave absorber by carbonization of pre-magnetized natural wood fibers. J. Bioresour. Bioprod. 4 (1), 43–50.

Macossay-Torres, J. et al., 2015. A comparative study of polyurethane nanofibers with different patterns and its analogous nanofibers containing MWCNTs. Adv. Mater. Lett. 6 (9), 768.

Madrid, A.P.M. et al., 2019. Advances in additive manufacturing for bone tissue engineering scaffolds. Mater. Sci. Eng. C 100, 631–644.

Martins, A.M. et al., 2014. Electrically conductive chitosan/carbon scaffolds for cardiac tissue engineering. Biomacromolecules 15 (2), 635–643.

Nguyen, H.-L. et al., 2016. Mussel-inspired anisotropic nanocellulose and silver nanoparticle composite with improved mechanical properties, electrical conductivity and antibacterial activity. Polymers 8 (3), 102.

Qu, H. et al., 2019. Biomaterials for bone tissue engineering scaffolds: a review. RSC Adv. 9 (45), 26252–26262.

Qu, H., 2020. Additive manufacturing for bone tissue engineering scaffolds. Mater. Today Commun. 24, 101024.

Ramakrishna, S. et al., 2006. Electrospun nanofibers: solving global issues. Mater. Today 9 (3), 40–50.

Subbiah, T. et al., 2005. Electrospinning of nanofibers. J. Appl. Polym. Sci. 96 (2), 557–569.

Subramanian, A., Krishnan, U.M., Sethuraman, S., 2012. Axially aligned electrically conducting biodegradable nanofibers for neural regeneration. J. Mater. Sci. - Mater. Med. 23 (7), 1797–1809.

Wang, W. et al., 2019. Engineered 3D printed poly (ε-caprolactone)/graphene scaffolds for bone tissue engineering. Mater. Sci. Eng. C 100, 759–770.

Wibowo, A. et al., 2020. 3D printing of polycaprolactone–polyaniline electroactive scaffolds for bone tissue engineering. Materials 13 (3), 512.

Wickham, A. et al., 2016. Electroactive biomimetic collagen-silver nanowire composite scaffolds. Nanoscale 8 (29), 14146–14155.

Xu, C. et al., 2004. Aligned biodegradable nanofibrous structure: a potential scaffold for blood vessel engineering. Biomaterials 25 (5), 877–886.

Xu, T.-C. et al., 2021. High strength electrospun single copolyacrylonitrile (coPAN) nanofibers with improved molecular orientation by drawing. Chin. J. Polym. Sci. 39 (2), 174–180.

Yang, X. et al., 2020. Structural design toward functional materials by electrospinning: A review. E-Polymers 20 (1), 682–712.

Yin, Z. et al., 2010. The regulation of tendon stem cell differentiation by the alignment of nanofibers. Biomaterials 31 (8), 2163–2175.

Zhang, Z. et al., 2018. Electroactive Scaffolds for neurogenesis and myogenesis: Graphene-based nanomaterials. Small 14 (48), 1801983.

Zheng, S. et al., 2021. Chitin derived nitrogen-doped porous carbons with ultrahigh specific surface area and tailored hierarchical porosity for high performance supercapacitors. J. Bioresour. Bioprod. 6 (2), 142–151.